

Toward Modeling Phosphate Tellurate Glasses: The Devitrification and Addition of Gadolinium Ions Behavior

S. Rada,* M. Culea, and E. Culea

Physics Department, Technical University of Cluj-Napoca, 400641 Cluj-Napoca, Romania, and Faculty of Physics, Babes-Bolyai University of Cluj-Napoca, 400084 Cluj-Napoca, Romania

Received: June 12, 2008

Glasses in the $x\text{Gd}_2\text{O}_3 \cdot (100 - x)[7\text{TeO}_2 \cdot 3\text{P}_2\text{O}_5]$ system with $0 \leq x \leq 20$ mol % have been prepared using the melt quenching method. The influence of gadolinium ions on structural behavior of the phosphate tellurate glass has been investigated using infrared spectroscopy and density functional theory (DFT) calculations. The addition of gadolinium ions into the host glass matrix leads to an increase of the glass network polymerization due to the replacement of P–O–P bonds by the more resistant P–O–Te bonds having as result the improvement of the chemical durability of the glass. The structural evolution of the studied glasses with the gradual increase of the gadolinium oxide content up to 20 mol % could be explained by considering that the excess of oxygen may be accommodated by the conversion of some orthophosphate structural units into metaphosphate or/and pyrophosphate units. X-ray diffraction and IR spectra revealed that heat treatment of the samples also causes an increase of the glass network polymerization for heat treatment times, t , up to 36 h, while for $36 \text{ h} > t \geq 48 \text{ h}$ showed a drastic structural modification which lead to the apparition of the $\text{Te}_4\text{P}_2\text{O}_{13}$ crystalline phase. DFT calculations show that tellurium atoms occupy two different sites in the proposed model. In the first case the tellurium atom is coordinated with four oxygen atoms giving a trigonal bipyramide arrangement, while in the second case the tellurium atom is coordinated with three O atoms. The calculated IR absorption spectrum of the proposed model for phosphotellurite glasses is in good agreement with the experimental absorption data.

1. Introduction

The structural origins of glassy materials are very important to science today.¹ Phosphate glasses have attracted greater attention because of the strong glass forming character, simple structure,² and high ionic conductivities.^{3,4} However, their relatively poor chemical durability makes them generally unsuitable for practical applications.⁵ Many studies show that the addition of halides or oxides of the alkali, alkaline earth, and transition metals can improve the chemical durability of the tellurite glasses.^{6,7} This may open new opportunities in different biological⁸ and electrochemical applications.^{9–11} Thus, to improve the chemical durability of the conventional phosphate glasses and to ensure their utilization in new technological and biological applications is of very high interest.^{12–14}

Tellurium dioxide, TeO_2 , is a conditional glass former. It is very difficult to form pure vitreous TeO_2 , and it has been suggested that this is due to the lone pair of electrons in one of the equatorial positions of the $[\text{TeO}_4]$ polyhedron. Tellurite glasses are high refractive index optical glasses possessing high levels of infrared transmission having potential applications as acoustic and optical materials used in laser technology or as photochromic materials.¹⁵

For clarification, the structure of the binary tellurite glasses in some works are done by analyzing the basic structural units whereby $[\text{TeO}_4]$ trigonal bipyramid and $[\text{TeO}_3]$ trigonal pyramids are found in crystals^{16,17} and in glasses.¹⁸

A lone pair of electrons occupies one equatorial site of the Te sp^3d hybrid orbitals in the $[\text{TeO}_4]$ unit and also the apex of the sp^3 hybrid orbitals in the $[\text{TeO}_3]$ unit. The axial Te–O bonds

of the $[\text{TeO}_4]$ unit are little longer than the equatorials bonds. Several studies of tellurite glasses¹⁹ give some indications for additional O sites at distances larger than these typical Te–O bonds that are also known to from crystal structures.^{20,21} Previous reports show that by adding an alkali network modifier oxide such as Na_2O , the Te–O–Te network bridges are broken accompanied by the formation of nonbridging oxygen sites.^{22,23} The $[\text{TeO}_3]$ fraction increases at the expense of the $[\text{TeO}_4]$ units. The effect appears reduced for tellurite glasses modified by the conditional glass formers V_2O_5 ²⁵ and WO_3 .²⁶

The structure and the properties of the oxide glasses are dependent strongly on the nature and the concentration of the constituent oxides. Thus, as was mentioned previously, the addition of glass network modifier atoms causes the network to break. In tellurate glasses the modifier atoms seem to cause also the modification of the basic structural units, the $[\text{TeO}_4]$ trigonal bipyramids, and the $[\text{TeO}_3]$ trigonal pyramids with one of the equatorial position occupied by a lone pair of electrons.^{22,23} To understand more about this aspect, we have carried out the studies on $x\text{Gd}_2\text{O}_3 \cdot (100 - x)[7\text{TeO}_2 \cdot 3\text{P}_2\text{O}_5]$ glasses with $0 \leq x \leq 20$ mol % Gd_2O_3 .

Despite some previous reports, the structure of $\text{TeO}_2\text{–P}_2\text{O}_5$ glasses is still subject of discussion.²⁴ The purpose of this paper was to approach the structure of glasses obtained in the $7\text{TeO}_2 \cdot 3\text{P}_2\text{O}_5$ system using the infrared spectroscopy and density functional theory (DFT) calculations. By combination of the calculated IR spectra for different clusters which can form the continuous random network of the glass with the experimental spectrum, we aim to define and to understand the structure of the $7\text{TeO}_2 \cdot 3\text{P}_2\text{O}_5$ phosphate tellurate glass network. In addition, to improve the chemical durability of the conven-

* To whom correspondence should be addressed. E-mail: Simona.Rada@phys.utcluj.ro.

tional phosphate tellurate glasses, the devitrification and the structural effects of increasing the gadolinium ions content in the $x\text{Gd}_2\text{O}_3 \cdot (100 - x)[7\text{TeO}_2 \cdot 3\text{P}_2\text{O}_5]$ system were studied.

2. Experimental Section

The binary $7\text{TeO}_2 \cdot 3\text{P}_2\text{O}_5$ glasses were prepared by mixing together specific weights of TeO_2 and H_3PO_4 in ceramic crucibles. The crucible was transferred to a furnace for 60 min at 1100 °C. The glassy sample was subject to heat treatment applied at 500 °C for 16, 36, and 48 h, respectively.

The samples were analyzed by means of X-ray diffraction using a XRD-6000 Shimadzu diffractometer, with a monochromator of graphite for the Cu K α radiation ($\lambda = 1.54 \text{ \AA}$) at room temperature.

The structure of the glasses was investigated by infrared spectroscopy using the KBr pellet technique. The IR spectra were recorded in the range 400–1400 cm^{-1} using a JASCO FT-IR 6200 spectrophotometer.

The starting structures have been built using the graphical interface of Spartan 04²⁷ and preoptimized by molecular mechanics. The geometries were optimized at the B3PW91/CEP-4G/ECP level of theory using the Gaussian 98 package of programs.²⁸ For tellurium atoms the effective core potential (ECP) proposed by Hay and Wadt²⁹ has been adopted together with the associated basis set. The same ECP has been tested in the framework of DFT by carrying out B3PW91 calculations.

Dangling bonds of outer atoms of the models were saturated with hydrogen atoms. For each sample of phosphotellurite glass the structural geometry was completely optimized, and the vibrational frequencies and the IR absorption intensities were calculated for the equilibrium geometry.

Frequency analysis followed all optimizations in order to establish the nature of the stationary points found, so that all the structures reported in this study are genuine minima on the potential energy surface at this level of theory, without any imaginary frequencies. Accordingly, frequency calculations were performed to ensure that the stationary points were minima and to calculate infrared spectra. The calculated IR frequencies and intensities were transformed via the SWizard program³⁰ into simulated IR spectra using Lorentzian functions with half-widths of 15 cm^{-1} .

3. Results and Discussion

3.1. Structural Properties of the $7\text{TeO}_2 \cdot 3\text{P}_2\text{O}_5$ Glass. FT-IR spectrum of the $7\text{TeO}_2 \cdot 3\text{P}_2\text{O}_5$ glass for the 400–1400 cm^{-1} wavenumber range is shown in Figure 1a. The obtained IR bands and their assignments can be summarized as follows:

(i) The band located at about 530 cm^{-1} is attributed to the deformation modes of P–O bonds from the $[\text{PO}_4]$ groups.³¹

(ii) The large band centered at $\sim 625 \text{ cm}^{-1}$ is assigned to the stretching mode of $[\text{TeO}_4]$ trigonal bipyramidal with bridging oxygens.²² The shoulder located at about 750 cm^{-1} indicates the presence of $[\text{TeO}_3]$ units.³²

(iii) The band centered about 994 cm^{-1} can be due to $[\text{PO}_4]$ of orthophosphate groups vibrations. The position of the band from $\sim 1100 \text{ cm}^{-1}$ corresponds to the vibrations of PO_2 of metaphosphate groups. The band centered at about 1175 cm^{-1} is assigned to the PO_2 symmetric stretching mode and the P–O–P of $[\text{PO}_4]$ tetrahedral sharing corners. The shoulder near $\sim 900 \text{ cm}^{-1}$ is assigned to the asymmetric stretching mode.^{33,34}

The experimental FT-IR spectrum of the $7\text{TeO}_2 \cdot 3\text{P}_2\text{O}_5$ glass shows that the glass structure is made up mainly of trigonal bipyramidal $[\text{TeO}_4]$ groups with a lone pair of electrons, the

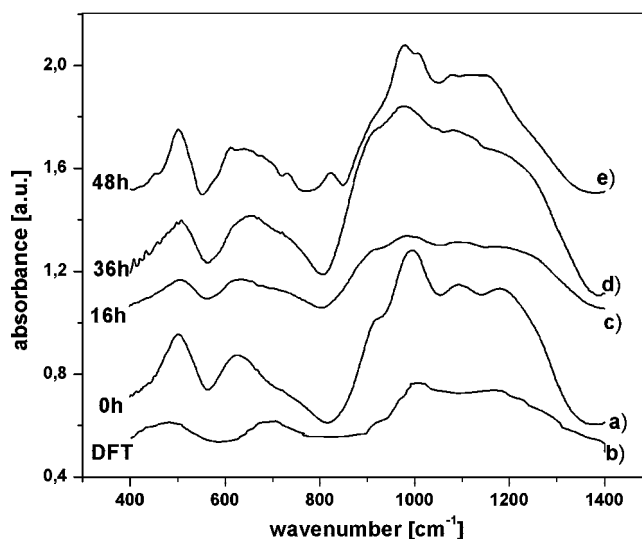


Figure 1. FT-IR spectra of the (a) untreated, (b) simulated, (c) 16-h treated, (d) 36-h treated, (e) 48-h treated for $7\text{TeO}_2 \cdot 3\text{P}_2\text{O}_5$ glass.

tetrahedral phosphate anion $[\text{PO}_4]$, and a small content of tetrahedral $[\text{TeO}_3]$ units.

The IR data were used in the present research in order to compute a possible structural model of the $7\text{TeO}_2 \cdot 3\text{P}_2\text{O}_5$ glass. Similar methodology has previously been reported to study other glasses.^{35–37} The simulation method used is able to provide a realistic description of the phosphate tellurate network structure as it predicts the formation of rings and cages which consist of 4-fold coordinated Te atoms (trigonal bipyramids $[\text{TeO}_4]$ where all the O atoms form bridging bonds with the environment), 3-fold coordinated Te atoms (trigonal $[\text{TeO}_3]$ pyramids where one of the O atoms is nonbridging, a second one forms O=Te double bond, and the other two O atoms form bridging bonds with the environment), and $[\text{PO}_4]$ units.^{38,39}

In general, we notice a good agreement between the experimental and calculated values of the lengths of the Te–O and of P–O bonds in the characteristic structural units (1.9–2.1 Å for the length of Te–O bond and 1.66–1.73 Å for the length of P–O bond). The calculated Te–O and P–O bond lengths in the $[\text{TeO}_4]$, $[\text{TeO}_3]$, and $[\text{PO}_4]$ groups agree well with the experimental data available in the literature (in particular obtained using neutron diffraction).^{40–42}

It is known that tellurate structures containing tetravalent Te could contain $[\text{TeO}_3]$ trigonal pyramids, TeO_{3+n} polyhedron with three short distances ranging from 1.86 to 1.95 Å, or $[\text{TeO}_4]$ disphenoids, each having a well defined $5s^2$ lone pair.⁴³ Higher-order TeO_n polyhedron are equally well found with $n = 5$ and 6, but with fifth and/or sixth Te–O distance at values larger than 2.7 Å, lower than the sum of the van der Waals radii for Te and O (3.58 Å). It is known that the Te lone pair occupies a volume that is comparable to that of an O ion.⁴⁴

The Te–O bond lengths in the TeO_n polyhedron of our model are ranged from 1.94 to 2.50 Å. These bonds are subdivided into two groups: short bonds (1.85–2.1 Å) and long bonds (2.30–2.57 Å).⁴⁴ Te^{4+} is the lone-pair cation and lone-pair electrons occupy a nonbonding orbital that is stereochemically active and can be regarded as an additional ligand completing the coordination polyhedron. In addition to the lone-pair cations, oxygen ions having low coordination numbers also help to open up the crystal structures.

There are two types of Te atoms in our model (Figure 2), namely:

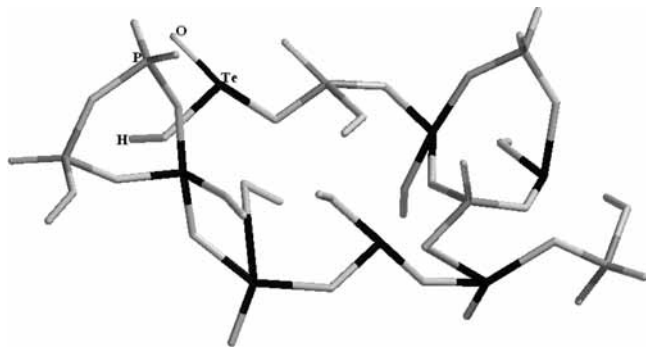


Figure 2. Optimized structure of the model for the binary $7\text{TeO}_2 \cdot 3\text{P}_2\text{O}_5$ glass.

(i) Tellurium is in tetragonal coordination. Three bonds have short interatomic distances (1.97–2.09 Å), and the fourth one has a longer interatomic distance (2.32 or 2.50 Å). The long Te–O bond distances are longer than the Te–O covalent bond (2.15 Å) but significantly shorter than the sum of the Van de Waals radii (3.58 Å). The mean Te–O distances 2.12–2.16 Å are comparable to the Te–O covalent bond distance (2.15 Å), and the tellurium atoms are strongly bonded to four oxygen atoms giving a trigonal bipyramide arrangement. This geometry of the Te^{4+} ions shows an asymmetric coordination due to the stereochemically active lone-pair electrons. Similar distorted tellurium coordination geometry has also been observed in iron tellurite halide compounds with three shorter bond distances (1.89–1.94 Å) and a longer one (2.49 Å).⁴⁵

(ii) Tellurium site is coordinated to three O atoms. All the Te–O distances are comparable to those Te–O bond distances from the $[\text{TeO}_3]$ units (1.81–2.03 Å).^{46,47}

For some $[\text{PO}_4]$ groups the lengths of the P–O bonds are somewhat longer than the P–O covalent bond but significantly shorter than the sum of the van der Waals radii (2.32 Å), suggesting an asymmetrical coordination in the tetrahedral $[\text{PO}_4]$ units.

The quantum chemical calculations of the IR absorption spectra reveal that the proposed model for phosphate tellurate glass network is in good agreement with the experimental IR absorption spectra (Figure 1b). The evolution of the vibrational spectrum of the proposed model is important for understanding the broadening effect of the glasses from the experimental FT-IR spectrum. Our results show that the Te–O and P–O stretching vibration region of the proposed model is similar to the same region of the glass. Then, the vibrational modes corresponding to the $[\text{PO}_4]$, $[\text{TeO}_3]$, and $[\text{TeO}_4]$ geometries are significantly broadened in the disordered phase. We also suggested that the proposed model is the basic building block of the $7\text{TeO}_2 \cdot 3\text{P}_2\text{O}_5$ glass. By comparison of the theoretical and experimental data, we conclude that the performance of the method/basic sets used for the prediction of the structural data and vibrational modes is good.

In brief, the vibrations of the massive $[\text{PO}_4]$ units can be coupled each other via $[\text{TeO}_3]$ and $[\text{TeO}_3]$ groups and oneself. This leads to the splitting of the bridge modes and a multiplication of the number of these bands.

3.2. Structural Properties of the $7\text{TeO}_2 \cdot 3\text{P}_2\text{O}_5$ Glass Ceramics. To understand the data of the theoretic IR spectrum concerning the vibrations of the massive $[\text{PO}_4]$ units, the glassy sample was subject to heat treatment and the doping with gadolinium ions.

The X-ray diffraction patterns did not reveal any crystalline phase in the treated samples up to 36 h. By increasing the

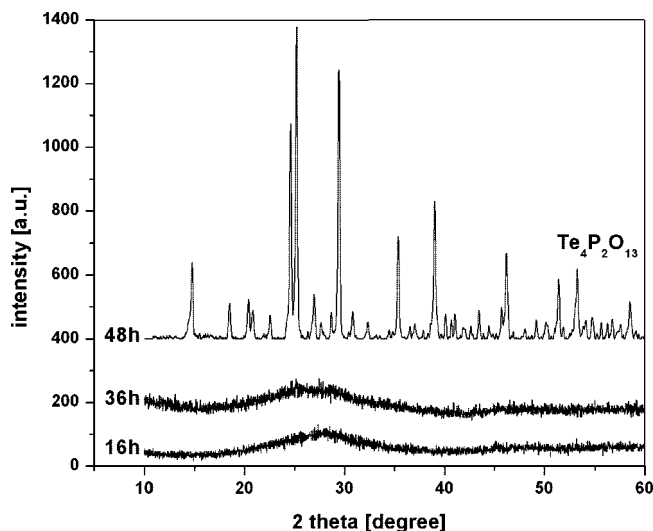


Figure 3. X-ray diffraction patterns for heat-treated $7\text{TeO}_2 \cdot 3\text{P}_2\text{O}_5$ samples.

treatment time from 36 to 48 h, the $\text{Te}_4\text{P}_2\text{O}_{13}$ crystalline phase was detected in the samples (Figure 3).

The FT-IR spectra of glass ceramics samples are reported in parts c–e of Figure 1. The heat-treated glass matrices show some changes of the FT-IR spectra with the increase of the treatment time. The absorption bands from the FT-IR spectra and their assignments can be summarized as follows:

(i) The band constituted from two characteristic features at ~ 625 and ~ 741 cm^{-1} (for the samples heat treated for ≤ 36 h) splits into four components located at ~ 605 , 653, 700, and 730 cm^{-1} (for the samples heat treated for 48 h). These bands were assigned to the Te–O bending and stretching vibrations in $[\text{TeO}_4]$ units. A new peak appears at ~ 820 cm^{-1} , and it is attributed to the $[\text{TeO}_3]$ units.

(ii) The shoulder centered at about 913 cm^{-1} shifts to 873 cm^{-1} , and it corresponds to the stretching of the P–O in pyrophosphate units.⁴⁷

(iii) The band centered at ~ 994 cm^{-1} (for the samples heat treated for ≤ 36 h) splits into two new bands located at 974 and 1008 cm^{-1} (for the samples heat treated for 48 h). These can be due to the vibrations of the $[\text{PO}_4]$ of orthophosphate groups.

(iv) The position of the band from ~ 1100 cm^{-1} was found to be shifted toward smaller wavenumber, namely, 1080 cm^{-1} , and its intensity decreases. This can be due to the vibrations of the PO_2 units of metaphosphate groups.⁴⁸ The appearance of the shoulders at ~ 730 cm^{-1} is also due to the presence of PO_2 units which are typical of the P_2O_7 groups.

(v) The prominent band located at about 1190 cm^{-1} was assigned to the stretching of the P=O bonds and shifts to ~ 1155 cm^{-1} .

The intensity of the absorption band located at about 994 cm^{-1} decrease dramatically for a heat treatment time, t , of 16 h and after that increase for higher t values. The evolution of this absorption band (assigned to $[\text{PO}_4]$ of the orthophosphate groups) suggests an increase of the degree of polymerization of the glass network for $t = 16$ h followed by a decrease for higher t values.

The IR data show that by increasing the heat treatment time of the samples a significantly different shape of the IR spectrum for 48 h compared to that for the samples heat treated for 16 and 36 h appears, namely, the features at ~ 625 and ~ 741 cm^{-1} (for the samples heat treated for ≤ 36 h) split into four components located at ~ 605 , 653, 700, and 730 cm^{-1} (for the

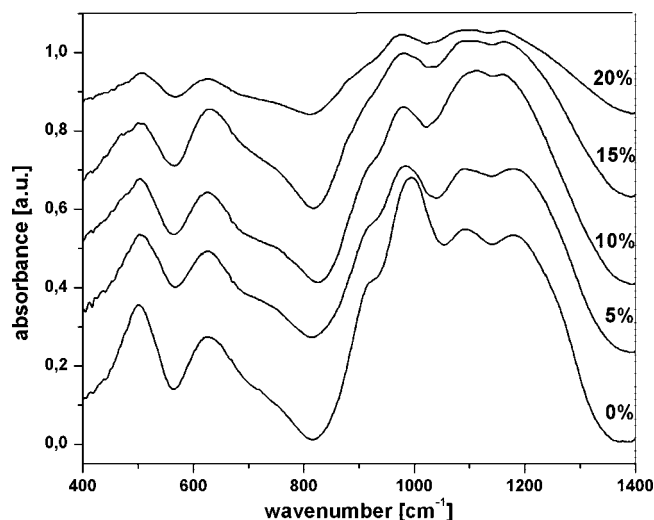


Figure 4. FT-IR spectra of the $x\text{Gd}_2\text{O}_3(100 - x)[7\text{TeO}_2 \cdot 3\text{P}_2\text{O}_5]$ glass with $x = 0$ –20% Gd_2O_3 .

samples heat treated for 48 h), and the band centered $\sim 994 \text{ cm}^{-1}$ (for the samples heat treated for $\leq 36 \text{ h}$) splits into two new bands located at 974 and 1008 cm^{-1} (for the samples heat treated for 48 h). These important changes of the IR features are due to the drastic structural change occurring between these samples due to the apparition of the $\text{Te}_4\text{P}_2\text{O}_{13}$ crystalline phase in the sample heat treated for 48 h, in agreement with the X-ray data.

3.3. Structural Properties of the $x\text{Gd}_2\text{O}_3 \cdot (100 - x)7\text{TeO}_2 \cdot 3\text{P}_2\text{O}_5$ Glasses. The examination of the FT-IR spectra of the $x\text{Gd}_2\text{O}_3(100 - x)[7\text{TeO}_2 \cdot 3\text{P}_2\text{O}_5]$ glasses with $x = 0$ –20 mol % (Figure 4) shows that the increase of the Gd_2O_3 content strongly modify the characteristic IR bands as follows:

(i) The band located at about $\sim 500 \text{ cm}^{-1}$ decreases with increasing the concentration of gadolinium ions and shifts to $\sim 508 \text{ cm}^{-1}$. As was previously mentioned, the presence of this band is attributed to the deformation modes of the P–O bonds from the $[\text{PO}_4]$ groups. This decrease can be due the replacement of the P–O–P bonds by the more resistant P–O–Te bonds

(ii) The intensity of the band from $\sim 630 \text{ cm}^{-1}$ increases by increasing the Gd_2O_3 content up to 15 mol % and after that decreases and shifts to $\sim 625 \text{ cm}^{-1}$. This band is attributed to the stretching vibrations in $[\text{TeO}_4]$ units.

(iii) The intensity of the band centered at $\sim 750 \text{ cm}^{-1}$ increases slowly with increasing the gadolinium ion content up to 15 mol %, while for higher contents the intensity of the band decreases slowly. This band is due to the Te–O stretching vibrations in $[\text{TeO}_3]$ units.

(iv) A new shoulder appears at about 873 cm^{-1} , which corresponds to the P–O vibrations in pyrophosphate units.

(v) The intensity of the band from $\sim 995 \text{ cm}^{-1}$ decreases with increasing the gadolinium ion content and shifts to $\sim 975 \text{ cm}^{-1}$. This band is due to the P–O stretching vibrations in orthophosphate units.

(vi) The intensities of the bands centered at about 1100 and 1195 cm^{-1} increase up to $x = 10\%$ and after that slowly decrease with increasing the gadolinium ion content. The position of these bands was found to be shifted toward lower wavenumbers with increasing gadolinium concentration (~ 1094 and 1161 cm^{-1} , respectively).

In brief, the increase of the gadolinium ion content of the samples leads to a variation of the intensities of the IR bands from $\sim 995 \text{ cm}^{-1}$ (due to orthophosphate structural units) to 1100

and 1195 cm^{-1} as was previously described (in paragraphs v and vi) suggesting an increase of the phosphate network polymerization. Such a behavior, namely, the increase of the polymerization degree of the structural units with increasing the rare earth ion content, was previously reported based on IR and XPS spectroscopy data for other glasses, too.^{49–52}

The stabilization of the phosphate structural units can be achieved by several metallic cations, namely, the gadolinium ions.⁵³ This should be the explanation for the formation of the vitreous phase when Gd_2O_3 is introduced into the host glass matrix. Then, the excess of oxygen can be supported into the glass network by the conversion of some orthophosphate structural units into metaphosphate or/and pyrophosphate units. Moreover, in the gadolinium phosphate tellurate glasses there is a replacement of the P–O–P bonds by the more resistant P–O–Te bonds leading to the improvement of the chemical durability.

4. Conclusion

Transparent glasses were easily obtained by cooling of the melts in air for all the studied compositions. The devitrification and the effects of addition of gadolinium ions to the $7\text{TeO}_2 \cdot 3\text{P}_2\text{O}_5$ glass were examined by infrared spectroscopy and quantum mechanical calculations.

Structural changes produced by the heat treatment of the samples consist in an increase of the degree of network polymerization for heat treatment times up to 36 h and a drastic structural modification due to the apparition of the $\text{Te}_4\text{P}_2\text{O}_{13}$ crystalline phase for 48 h.

The main results of the quantum chemical calculation of the structural model for the $7\text{TeO}_2 \cdot 3\text{P}_2\text{O}_5$ glass network show that the calculated IR absorption spectrum of the proposed model for phosphotellurite glasses is in good agreement with the experimental IR data. This procedure allowed us to assign most of the observed IR bands.

The FT-IR spectra of the phosphate tellurate glasses doped with gadolinium ions are modified generating a polymerization of the phosphate network. This compositional evolution of the structure could be explained by considering that the excess of oxygen may be accommodated by the conversion of some orthophosphate structural units into metaphosphate or/and pyrophosphate units. Moreover, in the gadolinium phosphate tellurate glasses, the $[\text{TeO}_3]$, $[\text{TeO}_4]$, and $[\text{PO}_4]$ units have a strong tendency to link with each other leading to the improvement of the chemical durability due to the replacement of the P–O–P bonds by the more resistant P–O–Te bonds.

References and Notes

- (1) Andriesh, A. M. *Phys. Appl. Non-Cryst. Semiconduct. Optoelectron.* **1997**, *36*, 17.
- (2) Brow, R. K. *J. Non-Cryst. Solids* **2000**, *263*, 1.
- (3) Rao, R. J.; Ganguli, M. *J. Non-Cryst. Solids* **1999**, *243*, 251.
- (4) Sidebottom, D. I. *Phys. Rev. B* **2000**, *61*, 14507.
- (5) Masingu, A.; Piccaluga, G.; Pnna, G. *J. Non-Cryst. Solids* **1990**, *52*, 29.
- (6) Pan, A.; Ghosh, A. *Phys. Rev. B* **2002**, *66*, 012301.
- (7) Brow, R. K. *J. Am. Ceram. Soc.* **1993**, *76*, 913.
- (8) Zhang, Y.; Huang, W.; Lu, K.; Zhao, Y. *J. Non-Cryst. Solids* **1993**, *112*, 136.
- (9) Martin, S. W.; Angell, C. A. *J. Am. Ceram. Soc.* **1984**, *C-148*, 67.
- (10) Hunter, C.; Ingram, M. D. *Phys. Chem. Glass.* **1986**, *27*, 51.
- (11) Das, S. S.; Baranwal, B. P.; Gupta, C. P.; Singh, P. *J. Power Sources* **2003**, *114*, 346.
- (12) Yilin, Y. Z.; Huang, W.; Lu, K.; Zhao, Y. *J. Non-Cryst. Solids* **1993**, *112*, 136.
- (13) Yu, X.; Day, D. E.; Long, G. J.; Brow, R. K. *J. Non-Cryst. Solids* **1997**, *215*, 21.

- (14) Mogus-Milankovic, A.; Gajovic, A.; Santic, A.; Day, D. E. *J. Non-Cryst. Solids* **2001**, 289, 204.
- (15) Kim, S. H.; Yoko, T. *J. Am. Ceram. Soc.* **1995**, 78, 1061.
- (16) Lindquist, O. *Acta Chem. Scand.* **1968**, 22, 87.
- (17) Galy, J.; Lindquist, O. *J. Solid State Chem.* **1979**, 27, 279.
- (18) Dimitriev, Y.; Dimitriev, V. *Mater. Res. Bull.* **1978**, 13, 1071.
- (19) Hoppe, U.; Yousef, E.; Russesl, C.; Neufeind, J.; Hannon, A. C. *Solid State Commun.* **2002**, 123, 273.
- (20) Hanke, K. *Naturwissenschaften* **1966**, 53, 273.
- (21) Mayer, H.; Pupp, G.; Kristallogr., *Z. Kristallgeom., Krystalphys., Kristallchem.* **1977**, 145, 321.
- (22) Sekiya, T.; Mochida, N.; Ogawa, S. *J. Non-Cryst. Solids* **1994**, 176, 105.
- (23) Pan, A.; Ghosh, A. *Phys. Rev. B* **1999**, 59, 899.
- (24) Ayasinghe, G. D. L. K. J.; Bandaranayake, P. W. S. K.; Souquet, J. L. *Solid State Ionics* **1996**, 447 (1), 86–88.
- (25) Frechero, M. A.; Quinzani, O. V.; Pettigrosso, R. S.; Villar, M.; Montani, R. A. *J. Non-Cryst. Solids* **2007**, 353, 2919.
- (26) Charton, P.; Gengembre, L.; Armand, P. *J. Solid State Chem.* **2002**, 168, 175.
- (27) Spartan 04, Wavefunction Inc., CA 92612.
- (28) Frisch, M. J.; Trucks, G. W.; Schlegel, H. B.; Scuseria, G. E.; Robb, M. A.; Cheeseman, J. R.; Zakrzewski, V. G.; Montgomery, J. A.; Stratmann, R. E.; Burant, J. C.; Dapprich, S.; Millam, J. M.; Daniels, A. D.; Kudin, K. N.; Strain, M. C.; Farkas, O.; Tomasi, J.; Barone, V.; Cossi, M.; Cammi, R.; Mennucci, B.; Pomelli, C.; Adamo, C.; Clifford, S.; Ochterski, J.; Petersson, G. A.; Ayala, P. Y.; Cui, Q.; Morokuma, K.; Rega, N.; Salvador, P.; Dannenberg, J. J.; Malick, D. K.; Rabuck, A. D.; Raghavachari, K.; Foresman, J. B.; Cioslowski, J.; Ortiz, J. V.; Baboul, A. G.; Stefanov, B. B.; Liu, G.; Liashenko, A.; Piskorz, P.; Komaromi, I.; Gomperts, R.; Martin, R. L.; Fox, D. J.; Keith, T. A. M.; Al-Laham, C. Y.; Peng, A.; Nanayakkara, M.; Chalocombe, P. M. W.; Gill, B.; Johnson, W.; Chen, M. W.; Wong, J. L.; Andres, C.; Gonzales, M.; Head-Gordon, E. S.; Replogle, J. A.; Pople, J. A. *Gaussian* 98, rev. A5; Gaussian Inc.: Pittsburgh, PA, 1998. Shih, P. Y. Yung, S. W. Chin, T. S. *J. Non-Cryst. Solids*, 127, 143 (1991).
- (29) Hay, P. J.; Wadt, W. R. *J. Chem. Phys.* **1985**, 82, 270.
- (30) Gorelsky, S. I. *SWizard*; Department of Chemistry, York University: Toronto, ON, 1999; <http://www.sg-chem.net>.
- (31) Bartholomew, R. F. *J. Non-Cryst. Solids* **1972**, 7, 221.
- (32) Rada, S.; Culea, E.; Rus, V.; Pica, M.; Culea, M. *J. Mater. Sci.* **2008**, 43, 3713.
- (33) Byun, J. O.; Kim, B. H.; Hong, S. K.; Jung, H. J.; Lee, S. W.; Izyneev, A. A. *J. Non-Cryst. Solids* **1995**, 190, 88.
- (34) Brow, R. K.; Tallant, D. R.; Myers, S. T.; Phifer, C. C. *J. Non-Cryst. Solids* **1995**, 191, 45.
- (35) Rada, S.; Culea, M.; Neumann, M.; Culea, E. *Chem. Phys. Lett.* **2008**, 460, 196.
- (36) Ispas, S.; Benoit, M.; Jund, P.; Jullien, R. *Phys. Rev. B* **2001**, 64, 214206.
- (37) Rada, S.; Culea, E.; Bosca, M.; Culea, M.; Muntean, R.; Pascuta, P. *Vibrational Spectrosc.* In press.
- (38) Tenney, A. S.; Wong, J. *J. Chem. Phys.* **1972**, 56, 5516.
- (39) Wong, J. *J. Non-Cryst. Solids* **1976**, 20, 83.
- (40) Iordanova, R.; Dimitrov, V.; Dimitriev, Y. *J. Non-Cryst. Solids* **1994**, 180, 58.
- (41) Abo-Naf, M.; Batal, F. H. E.; Azooz, M. A. *Mater. Chem. Phys.* **2002**, 77, 846.
- (42) Kumar, A.; Rai, S. B.; Rai, D. K. *Mater. Res. Bull.* **2003**, 38, 333.
- (43) Van der Lee, A.; Astier, R. *J. Solid State Chem.* **2007**, 180, 1243.
- (44) Galy, J.; Meunier, G.; Anderson, S.; Astrom, A. *J. Solid State Chem.* **1975**, 13, 142.
- (45) Becker, R.; Johnson, M. *J. Solid State Chem.* **2007**, 180, 1750.
- (46) Jiang, N.; Spence, J. C. H. *Phys. Rev. B* **2004**, 70, 184113.
- (47) Sokolov, V. O.; Plotnichenko, V. G.; Koltashev, V. V.; Dianov, E. M. *J. Non-Cryst. Solids* **2006**, 352, 5618.
- (48) Chahine, A.; Et-tabirou, M.; Elbenaisi, M.; Haddad, M.; Pascal, J. L. *Mater. Chem. Phys.* **2004**, 84, 341.
- (49) Anderson, G. W.; Compton, W. D. *J. Chem. Phys.* **1970**, 52, 6166.
- (50) Rada, S.; Pascuta, P.; Bosca, M.; Culea, M.; Pop, L.; Culea, E. *Vibrational Spectrosc.* In press.
- (51) Pascuta, P.; Pop, L.; Rada, S.; Bosca, M.; Culea, E. *J. Mater. Sci.* **2008**, 19 (5), 424.
- (52) Pop, L.; Culea, E.; Bosca, M.; Neumann, M.; Muntean, R.; Pascuta, P.; Rada, S. *J. Optoelectron. Adv. Mater.* **2008**, 10 (3), 619.
- (53) Radaev, S. F.; Simonov, V. I. *Sov. Phys. Crystallogr.* **1992**, 37, 484.

JP807089M